Appendix 1

The Structure of *E. coli* BtuF

in the B_{12}-bound and Substrate-Free Forms

Shortly after our structure of B_{12}-bound BtuF was published (1), Karpowich et al. published a structure of B_{12}-BtuF (also at 2.0 Å) as well as a model of apo-BtuF at 3.0 Å resolution (2). All three BtuF crystals grew from a solution of sodium acetate at pH=4.6 and had two molecules per asymmetric unit. Indeed, the arrangement within the asymmetric unit is nearly identical in the two B_{12}-containing crystals, although the space group is not the same. Both the space group and the arrangement within the asymmetric unit are different in the apo-BtuF crystals. While we used the cobalt atom at the center of the bound B_{12} to do a multi-wavelength anomalous diffraction experiment for phasing, Karpowich et al. made use of a seleno-methionine derivative of BtuF to solve their B_{12}-bound structure. Molecular replacement was then used to obtain phases for apo-BtuF. The data collection and refinement statistics reported by Karpowich et al. appear to be within the acceptable range, though the R_{free} reported for their 2.0 Å structure of B_{12}-bound BtuF (26.2 %) is significantly higher than ours (21.0 %).

The B_{12}- BtuF model of Karpowich et al. is basically identical to our model. The average rmsd between the models is 0.747 Å, which is comparable to the 0.760 Å rmsd between the two molecules in our asymmetric unit and the 0.552 Å rmsd between the two BtuF molecules in the Karpowich et al. asymmetric unit (Table 1). In fact, the rmsd between our A molecule and either Karpowich molecule is below this average and the bound B_{12} molecules superimpose upon alignment. The position of the corrin ring, phosphate tail and DMB ring are virtually identical. The arrangement of the corrin ring side chains appears to be somewhat more flexible, as the amide groups are oriented randomly, sometimes using the nitrogen and sometimes the oxygen atom to interact with the protein

Molecule 1	# residues	Molecule 2	# residues	rmsd (Å)	average rmsd (Å)
Borths A	244	Borths B	244	0.760	
Karpowich A	244	Karpowich B	244	0.552	
Apo A	244	Apo B	227	1.099	
Borths A	244	Karpowich A	244	0.666	
Borths B	244	Karpowich B	244	0.909	0.747
Borths A	244	Karpowich B	244	0.643	
Borths B	244	Karpowich A	244	0.770	
Apo A	244	Borths A	244	0.872	
Apo A	244	Borths B	244	0.907	1.051
Apo B	227	Borths A	244	1.164	
Apo B	227	Borths B	244	1.262	
Apo A	244	Karpowich A	244	0.845	
Apo A	244	Karpowich B	244	0.883	1.050
Apo B	227	Karpowich A	244	1.322	
Apo B	227	Karpowich B	244	1.151	

Table 1. Comparison of BtuF Crystal Structure Models. The rmsd was calculated between all possible pair wise combinations of the two B_{12}-bound BtuF molecules in the asymmetric unit from our work (Borths A and B), and Karpowich et al. (Karpowich A and B) plus the two apo-BtuF molecules in the asymmetric unit from Karpowich et al. (Apo A and B). Calculations were done in O.

or nearby water molecules. When the Karpowich B molecule is aligned with our A and B molecules, the position of the corrin ring, phosphate tail and DMB ring (and therefore the corrin ring side chains) of B_{12} do not overlap as well. However, residues lining the binding cleft, especially the large aromatic side chains, adjust their position to compensate. The phosphate tail region does not contact the protein main chain or side chains in either structure so no adjustment in BtuF is required to accommodate it. The rmsd between the Karpowich B molecule and our B molecule (0.909 Å) is higher than the average. This appears to result from changes in the relative orientation of the C-terminal sub-domain of our B molecule as the rmsd between our N-terminal sub-domain and that of the Karpowich B molecule is only 0.502 Å. Interestingly, when the N-terminal sub-

domains are aligned, the B_{12} molecules in the binding cleft do not superimpose. This further highlights the importance of the conformational flexibility of the C-terminal sub-domain in B_{12} binding and probably B_{12} release (see below).

Even though our structures are basically identical, there is a difference in the published secondary structure assignment. Where we identify five beta strands in the C-terminal domain, Karpowich et al. only identify four, omitting a short strand between their beta strand 6 and alpha helix 7. Though the strand is very short, we believe that there are clearly beta sheet type hydrogen bonds between it and the two neighboring strands, and so have classified it as a beta strand and part of the beta sheet in the C-terminal sub-domain. FhuD is an iron-siderophore binding protein that is homologous to BtuF and was used as a starting point for our model-building. FhuD has five beta strands in its C-terminal domain. It seems likely that the topology has not changed between these two related binding proteins but, instead, this particular strand has been shortened to make room for the much larger binding pocket of BtuF.

In addition to the structure of B_{12}-bound BtuF, Karpowich et al. also report a model of apo-BtuF. As expected, there is no large hinge or twist motion of one sub-domain relative to another like that observed for the apo form of the maltose binding protein (3). In fact, the rmsd between the apo BtuF molecules and any of the B_{12}-bound molecules is still less that 1 Å (except in the case of apo-BtuF molecule B alignments due to the fact that only 227 of 244 residues are included in that model (see below)). Instead, in the absence of B_{12}, there is a general increase in the mobility of the C-terminal domain

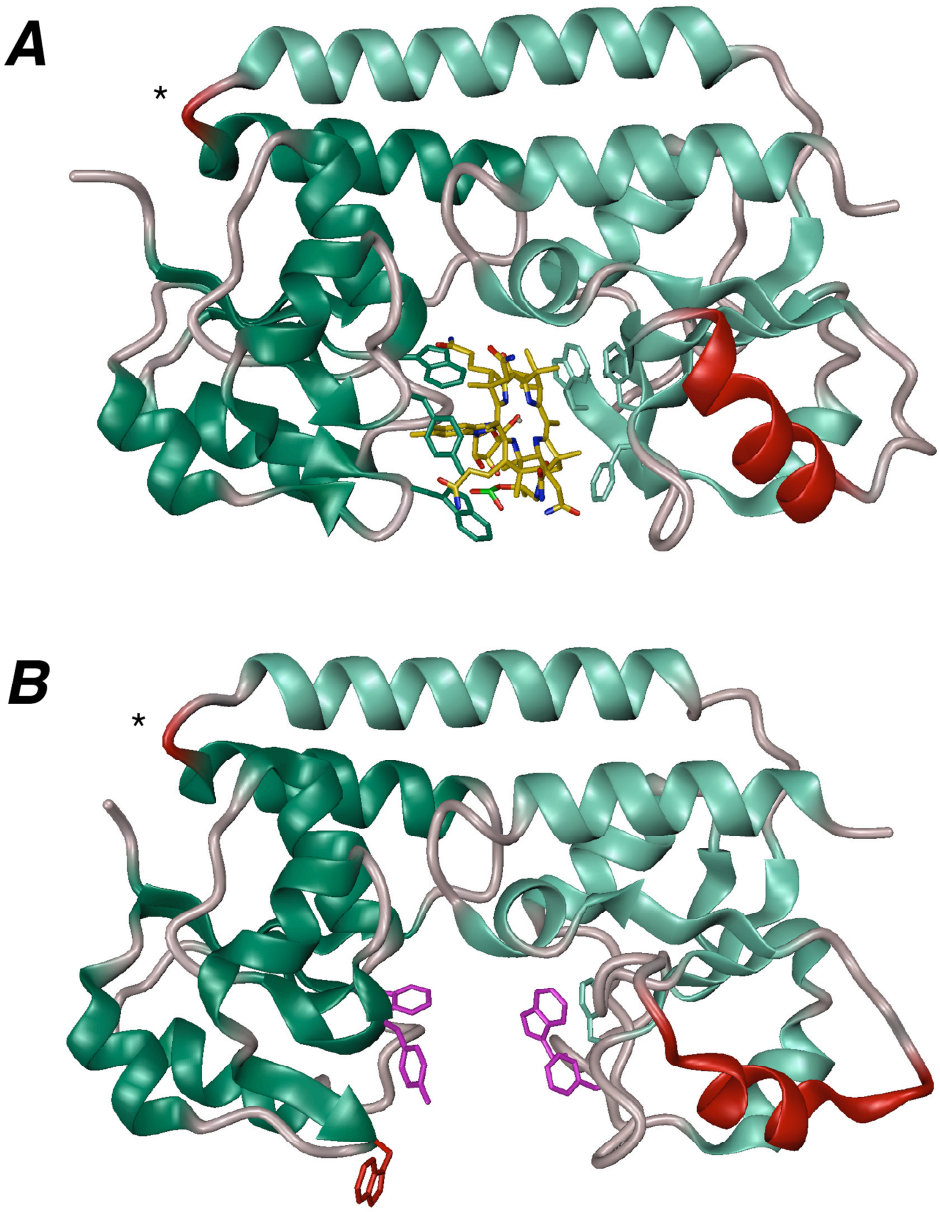

evidenced by elevated B-factors in that region and a rigid body rotation about Pro105 at the N-terminus of the backbone alpha helix (~10° upwards in the B molecule, less in A). This leads to a ~1 Å widening of the B_{12}-binding cleft (Figure 1). In addition, alpha helix 9 partially unwinds from both ends in the absence of B_{12}. Indeed, in apo-BtuF molecule B, the electron density in this region was so weak it could not be interpreted. In our

Figure 1. (previous page) Structure of BtuF in the presence and absence of vitamin B_{12}. The structure of (***A***) B_{12}-BtuF (1) and (***B***) apo-BtuF (2) are shown as ribbon diagrams. (***A***) The N-terminal domain is colored dark green while the backbone helix and C-terminal domain are light green. Alpha helix 9, in the nomenclature of Karpowich et al. is shown in red. Pro105, the residue that serves as pivot point for the rigid body rotation observed in the absence of B_{12}, is shown in red and marked with an asterisk. Side chains of the six aromatic residues contacting B_{12} in the binding cleft are shown in ball and stick and are colored dark or light green if they reside in the N or C-terminal domain, respectively. (***B***) Colors are as described for (***A***) except that the aromatic side chains are now colored to indicate the magnitude of their positional change in apo compared to B_{12} bound BtuF. W66 (the "cap") is shown in red and exhibits the largest change in position. Y50, W85, F168, and W196 are shown in magenta and exhibit a lesser degree of movement. F162 does not change position in

structure, this helix has the highest B factors and was the most difficult region to model, even though B_{12} was present. Within the B_{12} binding cleft, five of the six aromatic residues noted in our analysis have changed position in the apo relative to the B_{12} bound form (Figure 1B). In particular, W66, which sits like a cap over the B_{12} molecule, has swung away from the binding cleft.

Karpowich et al. hypothesize that one or more of these structural changes could participate in the release of B_{12} into the translocation pathway of the BtuCD transporter. The sensitivity of this region to the presence of B_{12} may mean that it is an important site of contact and/or communication between BtuF and BtuCD. Indeed, alpha helix 9 resides on a part of the BtuF molecule that we predict will interact with BtuC during the transport cycle (Chapter 2). But will the structural changes described for apo-BtuF alone be the same as those that occur when BtuF binds to BtuC and releases B_{12} into the BtuCD transporter? This is a much more complicated question because the mobility of these residues and indeed of the C-terminal lobe as a whole may be restricted (or perhaps enhanced) by their contact with BtuC. Other similar, or perhaps different, structural

changes may occur in response to rearrangements in BtuC coupled to hydrolysis of ATP by BtuD. The crystal structure of the BtuCD-F complex in various stages of the transport cycle as well as further biochemical analysis will be required to answer these questions.

References

1. Borths, E.L., K.P. Locher, A.T. Lee, and D.C. Rees, *The structure of* Escherichia coli *BtuF and binding to its cognate ATP binding cassette transporter*. Proc. Natl. Acad. Sci. USA, 2002. **99**(26): p. 16642-16647.

2. Karpowich, N.K., H.H. Huang, P.C. Smith, and J.F. Hunt, *Crystal structures of the BtuF periplasmic-binding protein for vitamin B_{12} suggest a funcationally important reduction in protein mobility upon ligand binding*. J. Biol. Chem., 2003. **278**(10): p. 8429-8434.

3. Quiocho, F.A. and P. Ledvina, *Atomic structure and specificity of bacterial periplasmic receptors for active transport and chemotaxis: Variation of common themes*. Mol. Microbiol., 1996. **20**(1): p. 17-25.